Title

Solving the quasi-static field model of the pulse-line accelerator; relationship to a circuit model

Author

Friedman, Alex

Publication Date

2005-10-14

Solving the quasi-static field model of the pulse-line accelerator; relationship to a circuit model*

Alex Friedman
LLNL and the Heavy Ion Fusion Virtual National Laboratory
October 14, 2005

The Pulse-Line Ion Accelerator (PLIA) is a promising approach to high-gradient acceleration of an ion beam at high line charge density [1, 2, 3, 4, 5, 6]. A recent note by R. J. Briggs [7] suggests that a "sheath helix" model of such a system can be solved numerically in the quasi-static limit. Such a model captures the correct macroscopic behavior from "first principles" without the need to time-advance the full Maxwell equations on a grid. This note describes numerical methods that may be used to effect such a solution, and their connection to the circuit model that was described in an earlier note by the author [8]. Fine detail of the fields in the vicinity of the helix wires is not obtained by this approach, but for purposes of beam dynamics simulation such detail is not generally needed.

In the axisymmetric limit, the continuity equation for charge (Briggs' eqn. 3) is:

$$\frac{\partial \lambda(z,t)}{\partial t} = -\frac{\partial I(z,t)}{\partial z} \ , \tag{1}$$

where $I(z,t)$ is the helix current and $\lambda(z,t)$ is the line charge density (charge per unit axial length along the helix). Here I can be thought of as charge per unit time passing through a cross-sectional plane cut across the wire itself, or (equivalently) as charge per unit time passing through a plane cut across either the sheath helix or the actual helix normal to its major axis; the former view makes the connection to a circuit model most obvious, while the latter is most natural for an axisymmetric description. Denoting the helix radius by a and the wire center-to-center spacing by s, the surface charge density on the helix sheet [Coul/m^2] is $\sigma = \lambda/2\pi a$, the azimuthal sheet current is $K_\theta = I/s$ [Coul/m/s], and the axial sheet current is $K_z = I/2\pi a$ [Coul/m/s]. Eq. 1 can be rewritten as:

$$\frac{\partial \sigma(z,t)}{\partial t} = -\frac{\partial K_z(z,t)}{\partial z} \ . \tag{2}$$

We will use Eq. 2 to advance the surface charge density $\sigma(z)$ to the future time level, and then compute the advanced-time electrostatic potential $\phi(r,z)$, and thus the electric field $E(r,z)$ that is needed in the interior of the helix to advance the simulation particles.

It is now possible to establish a correspondence with the circuit model of [8], which assumed (for convenience) one computational node per turn of the helix, that is, $\Delta z = s$. The σ_i at each node i can be integrated around the helix circumference and over an axial interval Δz to yield a charge Q_i. Then, those charges are related to the voltages on the set of nodes by the mutual capacitances:

$$\sum_j C_{ij} V_j = Q_i \ . \tag{3}$$

*Work performed under auspices of the U.S. D.O.E. by the University of California, Lawrence Livermore National Laboratory under Contract No. W-7405-ENG-48.

In the earlier note, a simpler local approximation (wherein the only nonzero elements of C_{ij} were the diagonal entries) was described, and it was the time derivative of this equation that was displayed, so that differences between currents, rather than charges, appeared in the formulation. Here we may precompute the capacitance matrix C_{ij} and then, at each time step, invert it to obtain the advanced-time voltages after we have computed the source terms by advancing the continuity equation, Eq. 2. Note that in the circuit model, the capacitance between each helix turn and the grounded outer pipe (with dielectric in between) plays a major role. Since the surface charge on the helix only establishes the jumps in E_r and not the actual potential values, the outer-wall boundary condition in the Poisson solution used to establish C_{ij} serves to set the diagonal elements C_{ii}, effectively the capacitances to ground.

For the purposes of a 1-D circuit model, knowledge of the capacitance matrix suffices. However, to advance the particles in an (r, z) or 3-D simulation it is necessary to obtain the electric field structure, and so (rather than using the capacitance matrix) a Poisson solution may well be carried out at each step, including the beam charge as a source term.

Briggs also relates the helix voltage $V(z, t)$ to the changing axial magnetic flux through the helix. Taking a path of integration in Faraday's law that passes inside the helix wire, extending axially by a distance Δz, the flux $\Phi(z, t)$ is encircled $\Delta z/s$ times, and the corresponding voltage change is:

$$\Delta V = -\frac{\Delta z}{s}\frac{\partial}{\partial t}\Phi(z, t) \ , \tag{4}$$

where the *total* flux through the helix (due to its own current and that of the primary strap) is:

$$\Phi(z, t) = \int_0^a B_z(r, z, t)\, 2\pi r\, dr \ . \tag{5}$$

In the continuum limit,

$$\frac{\partial}{\partial t}\Phi(z, t) = -s\frac{\partial V(z, t)}{\partial z} \ , \tag{6}$$

where we have transposed the left and right members to make it clear that we intend to use this equation to advance the flux in time. Actually, it is the magnetic field $\mathbf{B}(r, z, t)$, not the flux, that is desired at the advanced time, and initially it was not clear that the flux (which is a scalar function of the single spatial coordinate z) contains sufficient information to uniquely specify $\mathbf{B}(r, z, t)$ (which is a vector function of two spatial coordinates). The key realization in formulating this algorithm was the recognition that a set of N fluxes can uniquely specify a set of N current sources (corresponding to N turns of the helix, when $\Delta z = s$), and then those sources can be used to compute $\mathbf{B}(r, z, t)$ via the Biot-Savart law or other means.

It is a reasonable approximation to neglect the azimuthal component of the magnetic field, $B_\theta(r, z)$. This "skew" component is, in general, small in the vicinity of the beam, as can be seen via direct solutions of the Maxwell equations on a computational grid [4]. This corresponds to a set of current sources which are purely azimuthal (a coaxial set of circular hoops); at each computational node on the helix, this source is $K_\theta(z, t)\Delta z = (2\pi a/s)K_z(z, t)\Delta z = I(z, t)\Delta z/s$.

To make correspondence with the above-mentioned circuit model, the voltage change from node i to node $i + 1$ is related to the currents at the nodes by:

$$\Delta z \sum_j M_{ij}\frac{dK_\theta}{dt} = \frac{\Delta z}{s}\sum_j M_{ij}\frac{dI_j}{dt} = V_{i+1} - V_i \ . \tag{7}$$

In the circuit model, I_i is the current flowing between "voltage" nodes i and $i+1$. It is desirable to avoid two-cell difference expressions such as $V_{i+1}-V_{i-1}$ (which would be natural if all quantities were defined at the same set of axial locations) because of a concern that "decoupled" solutions might arise. That is, modes of oscillation wherein I is excited at odd-numbered nodes might diverge secularly from modes wherein the excitation is at even-numbered nodes. Also, finite differences based on smaller axial separations are more accurate. Note also that the well-known Yee discretization of finite-difference time-domain electromagnetics [9] employs "staggered" grids for E and B, so as to preserve important properties of the continuum equations in the finite-difference model. So motivated, we "offset" the axial locations of the currents from those of the voltages by half a cell. By examination of the governing equations, the "centering" of all other quantities can be developed. See Fig. 1.

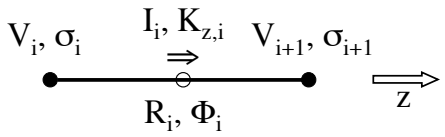

Figure 1: Spatial discretization along helix, showing locations of computational nodes.

When $\Delta z = s$, Eq. 7 describes the usual mutual-inductance relationship between the rates of change of the currents (I_j) through the turns j and the voltage change ($V_{i+1} - V_i$) across each inductor segment i. (Most of our work with the circuit model used the simpler local self-inductance coupling, $L_i = -M_{ii}$, which discards the nonlocal nature of the flux coupling.)

For any node spacing, equations 6 and 7 are clearly equivalent (in a finite-difference sense) when:

$$\sum_j M_{ij} I_j = -\Phi_i \ , \tag{8}$$

which is a familiar formula for mutual inductances (see, *e.g.*, [10]). In practice, the M_{ij} are precomputed before a simulation run begins time advancement, by setting I_j to unity for each j in turn, with the other currents zero, then computing $\mathbf{B}(r, z)$ and measuring the fluxes Φ_i at all axial nodes for each such configuration.

The sheath-helix model we are using does not restrict the node spacing Δz to be equal to s, and (as noted above) we wish to allow arbitrary zoning in the simulation code. Thus, we interpret the mutual inductances as coupling the magnetic fluxes through the tori associated with the individual computational zones with the currents in those zones. Note that we associate I_j with the current flowing in the helix wire through the plane $z = z_j$. I_j is *not* the total current flowing azimuthally in computational zone j on the helix, and *is* insensitive to zone size when sufficiently small zones are employed. To avoid confusion on this point, we rewrite Eq. 8 as:

$$2\pi a \sum_j M_{ij} K_{z,j} = -\Phi_i \ , \tag{9}$$

An algorithm

Clearly, many variations are available. Here, we outline one possibility. The algorithm consists of two main elements: a pre-computation phase to establish matrices that are needed during the

time-advance, and a series of actions that are taken at each computational time step, to advance the system state through an interval Δt. Denoting the time level (abbreviated "tl") of a quantity by a superscript, the step is described herein as an advance of the system from tl 0 to tl 1. The sheet current K_z is advanced from tl 1/2 to tl 3/2; it can be obtained at tl 1 by interpolation, as necessary for diagnostics or magnetic field computation. The overall procedure is formally a "leap-frog" advance, and is both "time centered" (in fact, reversible) and second-order accurate. At problem start-up, the current in the helix may be assumed to be zero, or a half-step may be taken to obtain values of K_z at tl 1/2.

Pre-computation

If only the voltages and currents on the helix are desired (an improved circuit model), precomputation of the capacitance matrix is appropriate; indeed, it may be desirable even in the general case. Refer to the discussion surrounding Eqn. 3. An enhanced model might also advance a set of particles in 1-D using applied fields computed via a separately precomputed Green's function that relates a unit voltage on the helix at $z = z_0$ to a voltage pattern $V(z - z_0)$ averaged over a nominal beam cross-section. Beam self forces might be modeled using a simple "$d\lambda/dz$" formulation, or (better) using yet another precomputed Green's function averaging across a nominal beam cross-section for both the charge-density and the force on a "slice" as a function of z.

In all cases, the mutual inductances of Eqn. 9 should be pre-computed.

Time advance

Enter the time step with the surface charge density on the helix σ defined at tl 0, and the axial sheet current K_z defined at tl 1/2.

(a) Advance the surface charge density on the helix using the continuity equation:

$$(\sigma_i^1 - \sigma_i^0)/\Delta t = -(K_{z,i}^{1/2} - K_{z,i-1}^{1/2})/\Delta z \ . \tag{10}$$

(b) For the simplest case of an improved circuit model, it suffices to associate charges $Q_i = \sigma_i \Delta z$ with each node, and solve Eqn. 3 for the V_j values. For the full simulation case, the surface charge induces a jump in the radial component of the electric field at the helix:

$$\epsilon_{\text{outer}} \left[\frac{\partial \phi^1(r,z)}{\partial r}\right]_{r=a^+} - \ \epsilon_{\text{inner}} \left[\frac{\partial \phi^1(r,z)}{\partial r}\right]_{r=a^-} = -\sigma^1(z) \ , \tag{11}$$

where ϵ is the dielectric constant (typically, constant in each subdomain of the problem), and "outer" and "inner" are with respect to the helix radius a, to account for the possibility of a change in ϵ at the helix radius. Here there are multiple possibilities:

(i) One could solve coupled Laplace equations with this jump in the gradient of ϕ as a constraint. This is not simply a matter of solving a Laplace equation with a Neumann boundary condition at the helix in each subdomain (*i.e.*, in the inner and outer regions), since only the jump in the gradient, and not the gradient itself, is known in advance. The additional constraint to be imposed is that the potential ϕ take on the same values at the helix nodes (that is, the computational nodes at $r = a$) in both subdomains.

(ii) Alternatively, we may "smear" the surface charge slightly by defining a charge density in the computational cell at the radius of the helix as $\rho = \sigma/\Delta r$, then solving a Poisson equation (including source terms from both helix charge, beam particles, stray electrons, and any other sources):

$$\nabla \cdot (\epsilon \nabla \phi^1) = -\rho^1 \ , \tag{12}$$

where the "stencil" for cells with radial index k corresponding to the helix radius might be:

$$\frac{\epsilon_{\rm outer}(\phi^1_{k+1}-\phi^1_k)-\epsilon_{\rm inner}(\phi^1_k-\phi^1_{k-1})}{\Delta r^2}+\left(\frac{\partial^2}{\partial z^2}\ {\rm term}\right)=-\frac{\sigma^1}{\Delta r}\ . \tag{13}$$

For an infinitesimally thin sheet, the axial second derivative is not needed since all z variations are "slow" in comparison to jump in the radial electric field; but in passing to a finite-thickness layer it is appropriate to include such as term, as indicated above. This conclusion was reached by drawing a Gaussian pillbox and noting that there may be a non-negligible electric flux $\mathbf{E}\cdot\hat{n}$ through the faces that separate adjacent computational nodes on the helix.

(c) From the solution $\phi^1(r,z)$ to the Poisson equation, the electric field $E^1(r,z)$ can be obtained via centered finite differences, and the voltages $V^1(z)$ at the computational nodes on the helix obtained as the corresponding values of ϕ^1. If particles are to be advanced in the immediate vicinity of the helix (within the last cell), it may be more appropriate to set the radial component of the electric field in the zones at $r=a$ to values computed via one-sided finite differences (since that component is discontinuous across the helix layer).

(d) Time-advance the magnetic flux through each helix node i using a finite-difference form of Eq. 6:

$$(\Phi^{3/2}_i-\Phi^{1/2}_i)/(\Delta t)=-s(V^1_{i+1}-V^1_i)/\Delta z\ . \tag{14}$$

(e) Obtain currents at the helix nodes from the magnetic fluxes by inverting the inductance matrix, Eq. 9.

(de′) Note that steps (d) and (e) may be combined, and introduction of the intermediary flux quantities Φ avoided, by substituting Eq. 9 into Eq. 14 to yield:

$$\frac{\Delta z}{s}\frac{2\pi a}{\Delta t}\sum_j M_{ij}(K^{3/2}_{z,j}-K^{1/2}_{z,j})=(V^1_{i+1}-V^1_i)\ , \tag{15}$$

where the sum involving the $K^{3/2}_z$ is to be segregated into the left member and the matrix inverted. In general, this is a dense matrix, though the elements diminish in magnitude away from the diagonal.

This approach is especially attractive when the helix ends in a terminating resistive line shaped so as to continue the helical pattern. In that case, the voltage drop per unit length has both inductive and resistive contributions, which add in series since the current in the inductor is exactly that in the resistor. The resistive voltage drop between nodes $i+1$ and i separated by a helix segment with a resistance per unit length R_i has two contributions:

$$\frac{\Delta z}{s}\frac{2\pi a}{\Delta t}\sum_j M_{ij}(K^{3/2}_{z,j}-K^{1/2}_{z,j})+2\pi a\Delta z R_i\frac{(K^{3/2}_{z,i}+K^{1/2}_{z,i})}{2}=(V^1_{i+1}-V^1_i)\ , \tag{16}$$

where again the terms in $K^{3/2}_z$ are to be segregated into the left member.

If it is desirable to obtain the K_z values at tl 1, a simple interpolation between quantities at tl 1/2 and tl 3/2 suffices; the required storage is trivial.

(f) Use the resulting sheet currents $K_{z,j}$ as sources in a magnetic field solving routine to obtain $\mathbf{B}^1(r,z)$ or $\mathbf{B}^{3/2}(r,z)$, if desired (necessary when electron orbits are being computed, or for improved accuracy in ion orbits, in the absence of an overwhelmingly strong applied magnetic field).

The "drive" can enter in any of several ways:

(i) If it is a current source, it replaces step (e) at node 1 using the prescribed input $I_{\rm input}(t)$.

(ii) If it is a voltage source, it enters as a boundary condition (internal boundary) in the Poisson solution of step (b), and the σ at that node may be ignored.

(iii) If it is via a transformer primary strap, itself driven by a current source, it becomes an extra "node 0" in the mutual inductance matrix; the flux Φ_0 is probably not of direct interest, unless the influence on the driving circuit is needed.

Discussion

The equations presented herein define a detailed one-dimensional model of wave propagation on the helix that can be coupled with a one-dimensional particle-in-cell model. The simplicity of such a model is attractive for development of insight and for rapid scoping studies; indeed, the simpler circuit model presented earlier lent valuable insight into the behavior of this novel system.

The circuit model from that earlier note was adapted by D. Grote for use in WARP, which allows multi-dimensional (2-D and 3-D) particle-in-cell simulations to be carried out, including detailed space charge fields. Such a more detailed model is valuable for detailed design and analysis studies. One reason it is necessary is that the programmatic goal is to employ very high line-charge densities, presenting a challenge to beam-end control. At the ends, the beam is not sufficiently paraxial for a reduced description to be reliable. Also, transverse and longitudinal motions are coupled at the ends; even when the effective longitudinal "synchrotron" frequency of individual particle motion is small, the shape of the beam-end evolves.

In the earlier circuit model, the effects of circuit "loading" by the beam were considered. For that purpose, it was necessary to infer an image current, and this was accomplished by introducing a time-varying surface charge that induced a voltage on the nodes via their capacitance to ground; the equation solved was:

$$\frac{\partial I}{\partial z} = -\mathcal{C}\frac{\partial V}{\partial t} - \frac{\partial I_b}{\partial z} = -\mathcal{C}\frac{\partial V}{\partial t} + \frac{\partial \lambda_b}{\partial t} \tag{17}$$

where $\mathcal{C}$ is the capacitance to ground per unit length, λ_b is the beam line charge density, and the latter equality follows from the continuity equation.

The WARP model improved on this by solving a Poisson equation that included the beam space charge as the only source term; the radial electric wall at the helix, which was the radial boundary of the simulation domain in that model, was used to infer the image charge induced by the beam. This, in conjunction with the field solution using the voltages on the helix as boundary values, led to a valuable "smoothing" of the coupling between the helix and the beam. The net effect was to greatly diminish the feedback of short wavelength modes in a way that the simple circuit model did not; thus the simple circuit model was, in that sense, pessimistic, especially with regard to beam-loading effects. The "enhanced" 1-D model proposed in this note would also capture the key smoothing effects on short wavelength feedback.

The WARP model also employed "sub-cycling" of the circuit equation advance, that is, use of a timestep size $\Delta t_{\rm circuit}$ to advance the current and voltage on the helix that was smaller than the $\Delta t_{\rm PIC}$ used to advance the particles and space-charge field. This can readily be accomplished in the

model described herein, since the charge density ρ^1 of the beam can be obtained by advancing the particle velocities to tl 1/2 and then the positions to tl 1, without knowledge of the helix voltages at intervening substeps. By interpolating between ρ^0 and ρ^1, an approximate charge density at each substep can be used in solving for ϕ while including the effects of circuit loading by the beam.

Treating the helix as a perfect conductor for the purpose of computing the image charges is only an approximation. If the helix turns are separated by a large enough pitch, the "inner" fields can leak through and induce images on the outer pipe. The best model to use is still under consideration.

Studies of electrical breakdown, field stress, and (for some situations) electron-cloud in the helix may require a detailed treatment of the wires and their surroundings, and for such purposes another treatment will be needed.

Acknowledgements

This note describes an algorithm devised following discussions on 2005-08-25 about the physics model with R. J. Briggs, D. P. Grote, J-L. Vay, W. Waldron, and S. S Yu. The author thanks Dave Grote for useful discussions that led to improvements in this note.

References

[1] R. J. Briggs, *et al.*, "Helical Pulseline Structures for Ion Acceleration," *Proc. 2005 IEEE / APS Particle Accelerator Conference* (Knoxville, TN, May 2005); available on Web at: http://snsapp1.sns.ornl.gov/pac05/ROAB005/ROAB005.PDF .

[2] A. Friedman, *et al.*, "Highly compressed ion beams for High Energy Density Science," *Proc. 2005 IEEE / APS Particle Accelerator Conference* (Knoxville, TN, May 2005); available on Web at: http://snsapp1.sns.ornl.gov/pac05/ROAB003/ROAB003.PDF .

[3] G. Caporaso, *et al.*, "Dispersion Analysis of the Pulseline Accelerator," *Proc. 2005 IEEE / APS Particle Accelerator Conference* (Knoxville, TN, May 2005); available on Web at: http://snsapp1.sns.ornl.gov/pac05/FPAT034/FPAT034.PDF .

[4] S. D. Nelson, *et al.*, "Electromagnetic Simulations of Helical Based Ion Acceleration Structures," *Proc. 2005 IEEE / APS Particle Accelerator Conference* (Knoxville, TN, May 2005); available on Web at: http://snsapp1.sns.ornl.gov/pac05/FPAT037/FPAT037.PDF .

[5] W. Waldron, *et al.*, "High Voltage Operation of Helical Pulseline Structures for Ion Acceleration," *Proc. 2005 IEEE / APS Particle Accelerator Conference* (Knoxville, TN, May 2005); available on Web at: http://snsapp1.sns.ornl.gov/pac05/FPAT029/FPAT029.PDF .

[6] Proc. *Workshop on Accel. Driven High Energy Density Physics*, LBNL, Oct. 26-9, 2004, J. J. Barnard, Ed.; available on Web at: http://hifweb.lbl.gov/public/hedpworkshop/toc.html .

[7] R. J. Briggs, "Electromagnetic fields of a helix, and related topics" (unpublished note, 2005-08-23 rev. 1; to be made an LBNL research note).

[8] A. Friedman, "Studies of the Pulse-Line Accelerator Using a Circuit Model," available as LLNL Report UCRL-TR-210492 (2005) or LBNL Report LBNL-58938 (2005).

[9] K. S. Yee, "Numerical Solution of Initial Boundary Value Problems Involving Maxwell's Equations in Isotropic Media," *IEEE Trans. Antennas Propagat.* **14**, 302-307 (1966).

[10] R. P. Feynman, R. B. Leighton, and M. L. Sands, *The Feynman Lectures on Physics*, p. 17-9 ff., Addison-Wesley, Reading, MA, 1964.